03-202

Environment Canada

Water Science and Technology Directorate

Direction générale des sciences et de la technologie, eau

Environnement Canada

Multicoponent Reactive Transport Modelling of Acid Neutralization Reactions in Mine Tailings

By:
J. Jurjovec, D. Blowes, C. Ptacek, K. Mayer

NWRI Contribution # 03-202

03-202

Multicomponent Reactive Transport Modelling of Acid Neutralization Reactions in Mine Tailings

Jasna Jurjovec, David W. Blowes, Carol J. Ptacek, and K. Ulrich Mayer

Abstract

Multicomponent reactive transport modelling was conducted to analyze and quantify the acid neutralization reactions observed in a column experiment. Experimental results and the experimental procedures have been previously published. The pore water geochemistry was described by dissolution and precipitation reactions involving primary and secondary mineral phases. The initial amounts of the primary phases ankerite-dolomite, siderite, chlorite and gypsum were constrained by mineralogical analyses of the tailings sample used in the experiment. Secondary gibbsite was incorporated into the model to adequately explain the changes in pH and concentration changes of Al in the column effluent water. The results of the reactive transport modelling show that the pH of the column effluent water can be explained by dissolution reactions of ankerite-dolomite, siderite, chlorite and secondary gibbsite. The modelling results also show that changes in Eh can be explained by dissolution of ferrihydrite during the experiment. In addition, the modelling results show that the kinetically limited dissolution of chlorite contributes the largest mass of dissolved Mg and Fe (II) in the effluent water, followed by ankerite-dolomite, which contributes substantially less. In summary, reactive transport modelling based on detailed geochemical and mineralogical data was successful to quantitatively describe the changes in pH and major ions in the column effluent.

NWRI RESEARCH SUMMARY

Plain language title

Prediction of metal release from mine wastes

What is the problem and what do scientists already know about it?

The oxidation of sulfide minerals contained in mine wastes leads to the release of acid and metals to the environment. A series of reactions controls the concentrations and rates at which the acid and metals are released and transported from the wastes. Oxidation of sulfide minerals leads to the initial release of acid and metals to pore waters in the waste piles. Neutralization reactions lead to removal of the acid and attenuation of many metals within the waste piles. If there is abundant neutralization capacity in the wastes, all of the acid produced from sulfide oxidation will be neutralized. In high sulfide wastes, however, the neutralization capacity of the wastes is often insufficient to neutralize the acid over the long term. In this case, acid will be released from the wastes. Low pH conditions promotes the release of dissolved metals. Abundant information is available on oxidation reactions. Less information is available on neutralization reactions and metal attenuation reactions.

Why did NWRI do this study?

There are many minerals that are naturally present in mine wastes which contribute to acid-neutralization reactions. Each of these minerals reacts at different rates and releases different elements to infiltrating pore waters. This study was conducted to obtain measurements of rates of reactions, and to incorporate the measured rates into a predictive model of acid and metal transport in mine wastes. Models of this type can be used to predict the long-term release of acid and metals from mine waste sites. In many cases, metals and acid will continue to be leached long after ore recovery is complete. Accurate models are required to optimize the design of waste impoundments and water treatment systems to protect water quality at mine sites.

What were the results?

A multicomponent reactive transport model was modified and applied to laboratory column data collected to evaluate acid neutralization reactions in mine tailings. The model results agreed closely to measured data. A series of mineral dissolution reactions contributed to acid neutralization in the column. In can be expected that at mine sites in Canada, multiple phases will contribute to acid neutralization reactions. The model developed is a first step in developing a generalized approach for predicting the contributions of multiple phases in neutralizing acid in mine wastes.

How will these results be used?

The results can be used to improve estimates of acid and metal release from mine sites over the long-term. The results can also be used to assist in the design of a remedial systems for mine sites.

Who were our main partners in the study?

University of Waterloo; University of British Columbia; Falconbridge Mining Company

Modélisation du transport de divers composés réactifs pour les réactions de neutralisation de l'acide dans des résidus miniers

Jasna Jurjovec, David W. Blowes, Carol J. Ptacek et K. Ulrich Mayer

Résumé

La modélisation du transport de divers composés réactifs a été effectuée pour analyser et quantifier les réactions de neutralisation de l'acide observées dans une expérience sur colonne. Les résultats expérimentaux et les méthodes expérimentales ont été publiées antérieurement. La géochimie de l'eau interstitielle a été étudiée grâce à des réactions de dissolution et de précipitation mettent en jeu des phases minérales primaires et secondaires. Les quantités initiales des phases primaires ankérite-dolomite, sidérite, chlorite et gypse étaient limitées par les analyses minéralogiques de l'échantillon de résidus utilisé pour l'expérience. De la gibbsite secondaire a été incorporée dans le modèle pour expliquer valablement les modifications de pH et les variations de concentration d'Al dans l'eau de l'effluent de la colonne. Les résultats de la modélisation du transport de divers composés réactifs montrent que le pH de l'eau de l'effluent de la colonne peut s'expliquer par des réaction de dissolution de l'ankérite-dolomite, de la sidérite, du chlorite et du gibbsite secondaire. Les résultats de la modélisation montrent également que les variation d'Eh peuvent s'expliquer par la dissolution du ferrihydrite lors de l'expérience. De plus, les résultats de la modélisation montrent que la dissolution du chlorite, limitée par la cinétique, contribue à la formation de la masse la plus importante de Mg et de Fe (II) dans l'eau de l'effluent, suivie par celle de l'ankérite-dolomite, qui y contribue sensiblement moins. En résumé, la modélisation du transport de divers composés, basée sur des données géochimiques et minéralogiques détaillées, a permis de décrire quantitativement les variations du pH et des principaux ions dans l'effluent de la colonne.

Sommaire des recherches de l'INRE

Titre en langage clair

Prévision de la libération de métaux par les résidus miniers

Quel est le problème et que savent les chercheurs à ce sujet?

L'oxydation de minéraux sulfurés contenus dans les résidus miniers entraîne le rejet d'acide et de métaux dans l'environnement. Une série de réactions détermine les concentrations et les vitesses auxquelles de l'acide et des métaux sont libérés et transportés à partir des résidus. L'oxydation des minéraux sulfurés provoque la libération initiale d'acide et de métaux dans l'eau interstitielle à l'intérieur des dépôts de résidus miniers. Les réactions de neutralisation conduisent à l'élimination de l'acide et à l'atténuation de nombreux métaux à l'intérieur de ces dépôts. Si la capacité de neutralisation dans les résidus est élevée, tout l'acide produit par l'oxydation du sulfure sera neutralisé. Cependant, dans les résidus à haute teneur en sulfure, la capacité de neutralisation des résidus est

souvent insuffisante pour neutraliser l'acide à long terme. De l'acide sera alors libéré par les résidus. Un faible pH favorise la libération des métaux dissous. Il existe une information abondante sur les réactions d'oxydation. Les renseignements sont plus rares en ce qui concerne les réactions de neutralisation et les réactions d'atténuation des métaux.

Pourquoi l'INRE a-t-il effectué cette étude?

De nombreux minéraux, qui sont naturellement présents dans les résidus miniers, contribuent aux réactions de neutralisation de l'acide. Chacun de ces minéraux réagit selon différentes vitesses et libère divers éléments dans l'eau d'infiltration interstitielle. La présente étude a été effectuée pour mesurer les vitesses des réactions et pour incorporer les valeurs ainsi obtenues dans un modèle de transport d'acide et de métaux dans les résidus miniers. Des modèles de ce type peuvent être employés pour prévoir la libération à long terme d'acide et de métaux à partir de sites de résidus miniers. Dans beaucoup de cas, les métaux et l'acide continueront à être lessivés longtemps après la fin de l'extraction du minerai. Des modèles exacts sont nécessaires pour optimiser la conception des systèmes de retenue des résidus et de traitement des eaux, destinés à protéger la qualité de l'eau aux sites miniers.

Quels sont les résultats?

Un modèle de transport de divers composés réactifs a été modifié et appliqué aux données obtenues sur colonne en laboratoire afin d'évaluer les réactions de neutralisation de l'acide dans les résidus miniers. Les résultats produits par le modèle étaient très proches des données mesurées. Une série de réactions de dissolution minérale ont contribué à la neutralisation de l'acide dans la colonne. On peut prévoir que, sur les sites miniers du Canada, de multiples phases contribueront aux réactions de neutralisation de l'acide. Le modèle mis au point est une première étape dans l'élaboration d'une méthode générale de prévision des contributions de phases multiples à la neutralisation de l'acide dans les résidus miniers.

Comment ces résultats seront-ils utilisés?

Les résultats peuvent servir à améliorer les estimations de la libération à long terme d'acide et de métaux à partir de sites miniers. Les résultats peuvent également être employés pour faciliter la conception d'un système de remise en état des sites miniers.

Quels étaient nos principaux partenaires dans cette étude?

Université de Waterloo; Université de Colombie-Britannique; compagnie minière Falconbridge

WATER RESOURCES RESEARCH, VOL. 40, W11202, doi:10.1029/2003WR002233, 2004

Multicomponent reactive transport modeling of acid neutralization reactions in mine tailings

Jasna Jurjovec and David W. Blowes
Department of Earth Sciences, University of Waterloo, Waterloo, Ontario, Canada

Carol J. Ptacek
National Water Research Institute, Environment Canada, Burlington, Ontario, Canada
Department of Earth Sciences, University of Waterloo, Waterloo, Ontario, Canada

K. Ulrich Mayer
Department of Earth and Ocean Sciences, University of British Columbia, Vancouver, British Columbia, Canada

Received 2 April 2003; revised 4 June 2004; accepted 19 July 2004; published 10 November 2004.

[1] Multicomponent reactive transport modeling was conducted to analyze and quantify the acid neutralization reactions observed in a column experiment. Experimental results and the experimental procedures have been previously published. The pore water geochemistry was described by dissolution and precipitation reactions involving primary and secondary mineral phases. The initial amounts of the primary phases ankerite-dolomite, siderite, chlorite, and gypsum were constrained by mineralogical analyses of the tailings sample used in the experiment. Secondary gibbsite was incorporated into the model to adequately explain the changes in pH and concentration changes of Al in the column effluent water. The results of the reactive transport modeling show that the pH of the column effluent water can be explained by dissolution reactions of ankerite-dolomite, siderite, chlorite, and secondary gibbsite. The modeling results also show that changes in Eh can be explained by dissolution of ferrihydrite during the experiment. In addition, the modeling results show that the kinetically limited dissolution of chlorite contributes the largest mass of dissolved Mg and Fe (II) in the effluent water, followed by ankerite-dolomite, which contributes substantially less. In summary, reactive transport modeling based on detailed geochemical and mineralogical data was successful to quantitatively describe the changes in pH and major ions in the column effluent. *INDEX TERMS:* 1045 Geochemistry: Low-temperature geochemistry; 1829 Hydrology: Groundwater hydrology; 1806 Hydrology: Chemistry of fresh water; *KEYWORDS:* column experiment, acid mine drainage, acid neutralization mechanisms

Citation: Jurjovec, J., D. W. Blowes, C. J. Ptacek, and K. U. Mayer (2004), Multicomponent reactive transport modeling of acid neutralization reactions in mine tailings, *Water Resour. Res.*, *40*, W11202, doi:10.1029/2003WR002233.

1. Introduction

[2] During the last two decades, the field of reactive transport modeling of natural and contaminated systems has been developing rapidly, especially in its application to field-scale systems [*Steefel and Van Cappellen*, 1998]. For example, reactive transport modeling has previously been used to evaluate the mobility of contaminants in mine tailings [*Jaynes et al.*, 1984]. These reactive transport studies have explored the complex interactions between coupled processes in mill tailings environments for hypothetical cases and specific field sites.

[3] The limitations of predictive models and appropriateness of their use have been explored in a number of articles and editorials [*Bredehoeft and Hall*, 1995; *Bredehoeft and Konikow*, 1993; *Glynn and Brown*, 1996; *Konikow and Bredehoeft*, 1992; *Oreskes and Shrader-Frechette*, 1994]. One of the most significant problems with the predictive capabilities of models is an oversimplification of the conceptual model and/or the lack of appropriate input data to constrain the model. At most groundwater contamination sites there is less geochemical and hydrologic information known than may be desirable for contaminant transport modeling, because detailed hydrologic and geochemical studies are usually much too expensive to consider [*Glynn and Brown*, 1996].

[4] However, conditions in laboratory column experiments can be better controlled, and data from these experiments can be used in modeling studies to assess processes that affect the mobility of contaminants. Most recently, a number of studies have shown that reactive transport modeling can be used successfully to quantitatively assess reactive transport in well-constrained laboratory column experiments [e.g., *Appelo and Postma*, 1999a; *Guha et al.*, 2001; *Saiers et al.*, 2000].

[5] This paper presents results of multicomponent reactive transport modeling of a column experiment designed to study acid neutralization reactions in a mine tailings environment [*Jurjovec et al.*, 2002]. In this study, a pH 1 H_2SO_4

0043-1397/04/2003WR002233$09.00

solution, simulating acid mine drainage generated in unsaturated zones of tailings impoundments, was passed through a column containing fresh tailings from the Kidd Creek concentrator, located near Timmins, Ontario, Canada. The effluent was monitored to assess the change in pH and species as a function of time. The focus of the present study is to quantify and discern the acid neutralization reactions in isolation from acid generation reactions that took place in the column based on an expanded conceptual acid neutralization model proposed by *Morin et al.* [1988] and later refined by *Blowes and Ptacek* [1994]. The second objective of this study was to determine how well the results could match the measured concentrations of contaminants in the column effluent water when detailed and comprehensive information, gathered in the laboratory study, was available. The modeling study was well constrained by the large amount of geochemical, mineralogical and hydrologic information that has been gathered during the experimental study.

2. Model and Database Description

[6] MIN3P, a multicomponent reactive transport model, was developed by *Mayer et al.* [1999, 2002]. MIN3P is a general-purpose flow and reactive transport model. MIN3P is suitable for the simulation of processes that control the pore water chemistry in the column experiment conducted by *Jurjovec et al.* [2002]. In particular, the model allows the inclusion of aqueous complexation, hydrolysis, and redox reactions, as well as mineral dissolution-precipitation reactions.

[7] The thermodynamic database has been synthesized from the databases of WATEQ4F [*Ball and Nordstrom*, 1991] and MINTEQA2 [*Allison et al.*, 1990]. The equilibrium constants of minerals used in the simulations are summarized in Table 1. In addition, laboratory-derived rate constants and reaction orders for kinetically controlled reactions can be added to the MIN3P database. Alternatively, effective rate constants can be used. These rates are unique to the specific study. In this case, the surface area is incorporated into the effective rate constant. Reactive surface area measurements were not available for this study and effective rate coefficients were determined by calibration for most minerals (Table 2). For chlorite, a laboratory-derived rate expression and surface area normalized rate constants were used [*Lowson et al.*, 2004], and reactive surface area was obtained by model calibration.

3. Conceptual Model and Modeling Approach

[8] In this paper, four simulations are presented, which correspond to four conceptual models that were explored through a series of simulations that lead to the final interpretation. Initially, the conceptual model consisted of minerals determined on the basis of aqueous geochemical modeling of the experimental results described in detail by *Jurjovec et al.* [2002]. This series of minerals is consistent with the conceptual acid neutralization model proposed by *Morin et al.* [1988] and further refined by *Blowes and Ptacek* [1994]. According to the proposed conceptual acid neutralization model, a series of mineral precipitation-dissolution reactions controls the pH of pore water in mill tailings impoundments.

[9] This series of reactions can be subdivided into equilibrium and kinetically limited reactions [*Blowes and Ptacek*, 1994]. In the field, the reactions observed to be at equilibrium were dissolution of carbonates, and hydroxides, while aluminosilicate dissolution was observed to be kinetically limited [*Blowes and Ptacek*, 1994; *Dubrovsky et al.*, 1985; *Johnson et al.*, 2000; *Morin et al.*, 1988]. Minor quantities of minerals present in mine tailings control the pH of the pore water [*Blowes and Ptacek*, 1994; *Morin et al.*, 1988; *Morin and Cherry*, 1986].

[10] According to the proposed conceptual model, the pH of the pore water is maintained near neutral as long as a sufficient amount of calcite is present in the tailings and the flow rate is slow enough to attain equilibrium conditions:

$$CaCO_3 + H^+ \leftrightarrow Ca^{2+} + HCO_3^-$$

Because of high Fe(II) concentrations in the mine tailings pore water siderite may precipitate during calcite dissolution:

$$Fe^{2+} + HCO_3^- \leftrightarrow FeCO_3 + H^+$$

After all the calcite has dissolved, the pH will decrease and the pH of the pore water is controlled by siderite dissolution:

$$FeCO_3 + H^+ \leftrightarrow Fe^{2+} + HCO_3^-$$

From the onset of acidic conditions kinetically limited dissolution of aluminosilicates provides Al ions to the solution and gibbsite may precipitate:

$$Al^{3+} + 3\,OH^- \leftrightarrow Al(OH)_3$$

Upon depletion of siderite from the tailings, gibbsite dissolution will maintain the pH near 4.0. This is followed

Table 1. Equilibrium Constants for Primary and Secondary Minerals Included in the Investigation

Mineral	Log K
$Ca^{2+} + 0.6\,Fe^{2+} + 0.4Mg^{2+} + 2CO_3^{2-} \leftrightarrow$ ankerite-dolomite	18.16[a]
$Fe^{2+} + CO_3^{2-} \leftrightarrow$ siderite	10.45[b]
$Al^{3+} + 3H_2O - 3H^+ \leftrightarrow$ gibbsite	−8.11[c]
$Ca^{2+} + SO_4^- + 2H_2O \leftrightarrow$ gypsum	4.58[c]
$Fe^{3+} + 3H_2O - 3H^+ \leftrightarrow$ ferrihydrite	−4.891[c]

[a]Source: *Al* [1996].
[b]Source: *Singer and Stumm* [1970].
[c]Source: *Ball and Nordstrom* [1991].

Table 2. Effective Rate Constants and Rate Expressions Used in the Simulations

Phase	Rate Expression/ Effective Rate Constants for Steps 2–4
Chlorite	$\log R = -[9.79a_H^{0.49} + 13.00 + 16.79/a_H^{0.43}]$[a]
Ankerite-dolomite	6.8×10^{-7}[b]
Siderite	6.8×10^{-7}[b]
Gibbsite	9.0×10^{-7}[b]
Ferrihydrite	1.2×10^{-8}[b]
Gypsum (dissolution)	2.8×10^{-7}[b]
Gypsum (precipitation)	1.6×10^{-3}[b]

[a]Source: *Lowson et al.* [2004]. This rate expression was added to the MIN3P mineral database. Here a_H represents activity of hydrogen ion. Rate is expressed in mol (mineral) $m^{-2}\,s^{-1}$. The complete rate expression used in the code is rate = $S\,(\Sigma k_i\,a_i^n\,(1 - IAP/K_a))$, where S is surface area, k_i is rate constant of ion i, a_i is activity of ion i, n is reaction order, IAP is ion activity product, and K_a is the equilibrium constant.
[b]Effective rate constants reported in mol L^{-1} bulk s^{-1}; rate expression is rate = $k_{eff}\,(1 - IAP/K_a)$.

Table 3. Mineralogy of the Tailings Sample as Obtained by Image Analysis Study[a]

Mineral Class	Mineral Name	Formula	Weight Percent
Sulfides	pyrite	FeS_2	13.2
Sulfides	pyrrhotite	$Fe_{(1-x)}S$	1.2
Sulfides	chalcopyrite	$CuFeS_2$	0.5
Sulfides	sphalerite	ZnS	0.2
Silicates	chlorite	$(Mg, Fe)_3(Si, Al)_4O_{10}(OH)_2.(Mg, Fe)_3(OH)_6$	21.4
Silicates	amphibole	$W_{0-1}X_2Y_5Z_8O_{22}(OH, F)_2$[b]	0.5
Silicates	stiplnomelane	$K_{0.6}(Mg, Fe^{2+}, Fe^{3+})_6Si_8Al(O, OH)_{27}2\text{-}4H_2O$	<0.5
Silicates	albite	$Na\ Al\ Si_3O_8$	0.7
Silicates	muscovite	$KAl_2(AlSi_3O_{10})(OH)_2$	2.5
Silicates	quartz	SiO_2	49.1
Carbonates and Fe oxides	dolomite-ankerite	$CaMg(CO_3)_2$	3.1
Carbonates and Fe oxides	siderite and Fe-oxide	$FeCO_3$, FeO[c]	4.9

[a]From *Jurjovec et al.* [2002] (reprinted with permission from Elsevier). See *Jambor et al.* [1993].
[b]W = Na^+/K^+, X = Ca^{2+}, Na^+, Mn^{2+}, Fe^{2+}, Mg^{2+}, Li^+, Y = Mn^{2+}, Fe^{2+}, Mg^{2+}, Fe^{3+}, Al^{3+}, Ti^{4+}, and Z = Si^{4+}, Al^{3+}.
[c]The minerals were undistinguishable by image analyses.

by dissolution of iron oxyhydroxides. After the depletion of iron (oxy) hydroxides from tailings, the dissolution of aluminosilicates is the only process, which buffers the pore water pH.

[11] Several previous reactive transport modeling investigations of mine waste systems were conducted using an equilibrium approach. Examples of these investigations of acid neutralization reactions and metal attenuation at mine tailings sites include those of *Walter et al.* [1994] and *Liu and Narashimhan* [1989].

[12] In this study, the final solution of the problem was achieved in four steps. The initial conceptual model described above included only equilibrium reactions, which is consistent with the limitations of the previous generation of numerical models. Additional steps incorporated kinetically limited dissolution reactions. In the second step, gibbsite was removed from the conceptual model because its presence has not been verified by mineralogical studies. At the same time, dissolution of chlorite was introduced with the intention of identifying the reaction that simultaneously controls Fe, Mg, and Al concentrations. In addition, all the reactions were kinetically limited. The removal of gibbsite and introduction of chlorite in the second conceptual model did not result in adequate agreement between the simulated and observed Al concentrations. For this reason, gibbsite was reintroduced in the third conceptual model. At this point, the simulated concentrations of Fe and SO_4^{2-} at the beginning of the simulated experiment did not match the measured concentrations. Therefore no siderite precipitation was allowed in the fourth conceptual model. A more detailed discussion is provided in the results and discussion section.

[13] The minerals used in the conceptual model were either most soluble and/or most abundant in the Kidd Creek tailings, thereby these minerals are expected to affect the composition of the pore water most strongly. The complete mineralogy of the tailings used in the column experiment, as determined by *Jambor et al.* [1993], is shown in Table 3. The simplified mineralogical compositions of tailings used in steps 1, 2, 3 and 4 are summarized in Table 4.

[14] In Tables 3 and 4 and below, the mineral phases are classified as primary or secondary. This classification is consistent with the classification of tailings mineralogy proposed by *Jambor* [1994] and *Jambor and Blowes* [1998]. Primary phases are minerals initially present in the tailings material, before the beginning of the simulation. Secondary phases are minerals that were allowed to precipitate during the simulation when the solution reached equilibrium with respect to that particular phase. The masses of primary minerals used in the simulations are consistent with those measured using image analyses.

3.1. Physical Parameters

[15] A one-dimensional model domain was defined to simulate the laboratory column experiments. The length of the domain was set to 0.1 m, which is consistent with the length of the experimental column. The domain was discretisized into 100 elements. The inflow boundary was set as a second type boundary (Neumann condition) with a flow rate of 10.2 mL h^{-1}. This flow rate is consistent with the flow rate measurements made during a tracer experiment conducted prior to the laboratory column experiment. The outflow boundary was set as a first type boundary condition (Dirichlet condition) to reflect atmospheric pressure. The temperature was set constant at 25°C consistent with the temperature measured during the experiment, which varied minimally and was 25°C ± 0.5 except for two of the 97 measurements, which were 1.0°C lower.

[16] Column flow and solute transport parameters, namely dispersivity and velocity, were determined by modeling Cl concentrations measured during the tracer test, and gravimetrically measuring the flow rate. The modeled parameters were obtained from the leading edge of the breakthrough curve using the nonlinear least squares parameter optimization software CXTFIT [*Parker and van Genuchten*, 1994]. A dispersivity of 0.28 cm was obtained, which is consistent with observations of dispersivities in other column experiments [*Appelo and Postma*, 1999b]. The porosity and pore volume were calculated on the basis of gravimetric measurements of the column prior to the experiment. The porosity of the tailings in the column was 44 %, which is in good agreement with the average porosity of 0.4, observed in the field by *Al* [1996]. The column pore volume was 283 mL. The density of the tailings sample used in the calculations was 1.77 g/cm^3, as reported for the Kidd Creek tailings impoundment [*Al*, 1996].

3.2. Chemical Parameters

[17] The composition of water contained in the column before the initiation of the experiment was based on the

Table 4. Comparison of Initial Masses of Minerals Present in the Simulations and Mineralogical Analyses[a]

Mineral	Mineralogical Analysis	Initial Mass				Notes			
		Scenario 1	Scenario 2	Scenario 3	Scenario 4	Scenario 1	Scenario 2	Scenario 3	Scenario 4
Ankerite-dolomite	3	3	3	3	3	P	P	P	P
Siderite	5	4	4	4	4	P	P	P	P
Chlorite	24	-	24	24	24	-	P	P	P
Gibbsite	U	6.1	-	6.1	6.1	P	-	S	S
Ferrihydrite	U	0.01	0.01	0.01	0.01	P	P	P	P
Gypsum	0.5	0.5	0.5	0.5	0.5	P	P	P	P

[a]All mineral masses are reported in wt %. U, unidentified; P, primary; S, secondary.

composition of background solution (Table 5). The composition of water pumped through the column continuously was 0.1 M H_2SO_4, at pH value 1.

[18] The Kidd Creek tailings contain three primary solid solutions, which were used in the simulations: ankerite-dolomite, siderite and chlorite. In the simulations, these solid solutions were assumed to dissolve congruently, because MIN3P, at the present time, does not incorporate chemical changes of solids due to incongruent dissolution.

[19] Ankerite-dolomite composition in the simulations was simplified to $Ca(Fe_{0.6}Mg_{0.4})CO_3$, because the amount of Mn present in the ankerite-dolomite solid solution is only 4‰ and thus does not represent a major control on the system. In these simulations, siderite was assumed to be a pure phase due to its relatively low content of impurities. The stoichiometric solubility constant for Kidd Creek ankerite-dolomite, used in the simulations, was calculated by *Al* [1996]. The stoichiometric solubility constant was used in the simulations because no experimentally determined solubility constant was measured for ankerite-dolomite solid solution.

[20] The Fe/(Fe + Mg) ratio for chlorite in the Kidd Creek deposit is variable and ranges from 0.43 to 0.98 [*Slack and Coad*, 1989]. Microprobe analyses of Kidd Creek chlorite in the samples from the fringes of the stringer zone and massive sulfide ore, which best represent the chlorite found in the tailings, indicate a Fe/(Fe + Mg) ratio from 0.4 to 0.65 [*Slack and Coad*, 1989]. Most of the reported values were above 0.53. In the simulations, the ratio Fe/(Fe + Mg) of 0.65 was used. As in the case of ankerite-dolomite, congruent dissolution was assumed.

[21] A quasi-equilibrium approach was used for the step 1 simulation. This implies that effective dissolution-precipitation rate coefficients were chosen such that supersaturated conditions did not occur during the simulations at any time. It has been shown previously that such an approach may lead to numerical errors or convergence problems [*Chilakapati et al.*, 1998] due to additional stiffness introduced to the system of equations. However, the MIN3P code includes an adaptive time stepping scheme to deal with these issues. The code has also been tested against PHREEQC [*Parkhurst and Appelo*, 1999], which has the capability of describing dissolution-precipitation reactions as equilibrium reactions, for problems of similar nature as the one investigated here. Neither excessive CPU times, nor significant errors originated from the use of the quasi-equilibrium approach.

[22] For steps 2–4, effective kinetic rate constants were used for the ankerite-dolomite solid solution, siderite, gibbsite, ferrihydrite and gypsum (Table 2). A laboratory-derived rate expression determined by Lowson et al. (ANSTO, personal communication, 2002) for various buffered solutions at 25° between pH 3 and 10 was used for chlorite (Table 2).

[23] Simple empirical kinetic relationships provided improved fits of the simulated results to the observed data. The use of laboratory-derived rate expressions for all mineral phases, including the carbonate solid solution and siderite, was beyond the scope of the present study.

[24] The rates of gypsum dissolution and precipitation used in steps 2–4 differ significantly (Table 2). When the same rate coefficient was used for gypsum precipitation and dissolution, ($k_{eff} = 2.8 \times 10^{-7}$ mol L^{-1} s^{-1}), the simulation results indicated supersaturated conditions at the column outlet with respect to gypsum over a period of time, which was not observed in the column experiment. If a quasi-equilibrium approach was used for dissolution and precipitation of gypsum, concentration decreases of Ca and SO_4 as a result of gypsum depletion occurred much more rapidly than observed in the experiment. Possible explanations for the unusual behavior that gypsum appears to be dissolving slower than it precipitates may include (1) gypsum dissolution is inhibited by the presence of other mineral phases that have formed in the column during the experiment or (2) access of pore water to gypsum that was already present in the material prior to initiating the column experiment was limited.

[25] Modeling of kinetic reactions based on surface area normalized rate coefficients requires estimates of mineral surface area, which are difficult to measure [*White and Plummer*, 1990]. According to *White and Plummer* [1990], the greatest cumulative error in many kinetic models lies in the estimation of reactive surface areas in natural systems. In their study, *White and Plummer* [1990] compare a number of studies in which a kinetic approach was used.

Table 5. Initial Composition of Pore Water in the Column

Component	Initial Pore Water, mg L^{-1}		Input Solution, mg L^{-1}	
	Measured	Simulated	Measured	Simulated
Ca	686	764	<0.1	0
Fe	84.6	84.6	<5	0
Mg	18	18	<0.1	0
SO_4	10.0	10.0	104,000	10,400
Eh	279	279	494	400
pH	6.6	6.6	0.99	1
CO_3^{2-}	297	434	-	3.162×10^{-4}

In none of these studies, the surface areas used in simulations were consistent with geometric (calculated) or measured (BET) surface area. Therefore the term "reactive surface area" has been adopted widely, and is used in this study. Depending on the study, the reactive surface area can be smaller or larger than the geometric or BET surface areas. That is, there is no single explanation for these discrepancies. It is clear that the ambiguous term of "reactive surface area" needs to be dealt with in the future [*Lüttge et al.*, 2003].

[26] In this paper, the only surface area reported is that of chlorite because effective rates were used for all other minerals. In MIN3P, the surface area is included in the effective rate constant. That is, the surface area cannot be reported when the effective rate approach is used.

[27] The geometric surface area of chlorite was calculated on the basis of observations obtained from optical microscopy. Chlorite grains were found to be cylindrical in shape with average dimensions of 30 μm in diameter and length of 60 μm (Jambor, personal communication, 2000). The surface area of chlorite was calculated on the basis of the total tailings mass in the column, the mass fraction of chlorite in the sample [*Jambor et al.*, 1993], and an average density of 3.0 g cm^{-3}, reported for chlorites [*Klein and Hurlbut*, 1993]. The surface area of chlorite was calculated to be 16.9 m^2 L^{-1} of porous media. This calculation does not assume any surface roughness factor. The surface can increase by as much as 200 times for weathered silicates [*White and Plummer*, 1990] and for feldspars even up to a 1000 times [*Blum and Stillings*, 1995].

[28] In addition to chlorite grains described above, very small grains were found which resembled chlorite (Jambor, personal communication, 2000). Unfortunately, the grains were too small to be identified with certainty. This observation suggests that actual surface area of chlorite grains could potentially be larger. In the simulations presented below, the surface area of chlorite grains was 300 m^2 L^{-1} bulk porous medium. This surface area, which lies within the range for aluminosilicates recommended by *White and Plummer* [1990], was estimated by calibration in the second step to match the experimental pH curve at the second plateau at pH 4.

[29] The chlorite grains, remaining in the tailings material after the experiment, were analyzed by SEM to verify whether any signs of Fe-Mg-Al depletion or silica enrichment on the grain surface were detectable in the rims of the grains (Jambor, personal communication, 2000). The results of the SEM analysis were consistent with the observations of optical microscopy, whereby no "zoning" or alteration appeared to have been present in the chlorite grains after the completion of the experiment (Jambor, personal communication, 2000). In other words, the chlorite grains were homogeneous. This observation suggests that the assumption of congruent dissolution of chlorite may have been valid. However, the solids samples were not collected during the experiment, because collecting these samples would have substantially disrupted flow in the column. Such sampling would have enabled us to determine whether chlorite dissolution was also congruent at higher pH values. Observations of *Jambor* [2000] are consistent with observations of *Lowson et al.* [2004]. On the basis of production rate of ions in their laboratory dissolution study, they concluded that the dissolution of chlorite was congruent at low pH.

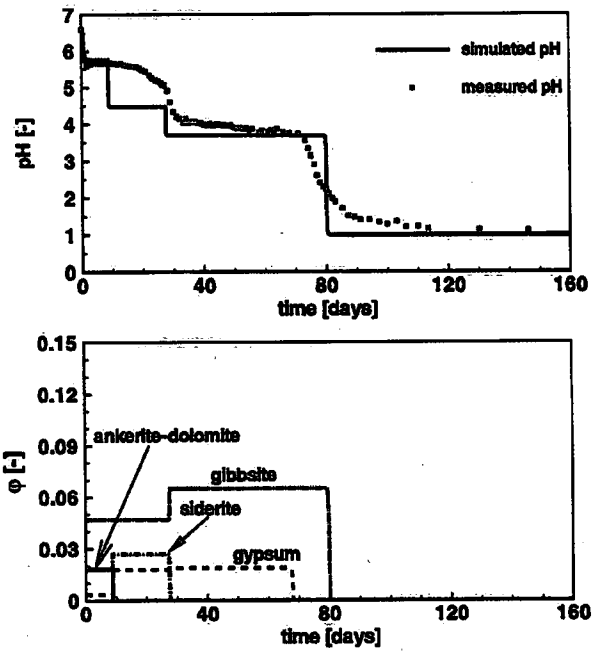

Figure 1. Step 1: Comparison of pH and abundance of minerals, expressed as volume fractions, at the outflow boundary of the column as a function of time.

[30] During the experiment, substantial amount of gas, originating from the column, passed through the sampling cell. Degassing was only observed during the first part of the experiment when pH was >4.0. Because neither hydraulic head nor the pressure measurements were collected in the column, degassing of CO_2 was not included in the simulations.

4. Results and Discussion

4.1. First Conceptual Model

[31] The first conceptual model consisted of the following primary buffering phases: ankerite, siderite, and gibbsite. In addition, primary gypsum was added to the conceptual model, due to its high solubility. The simplified mineralogy used in the simulation was based on mineralogical analysis (Table 3) and is summarized in Table 4. This initial conceptual model included only equilibrium reactions. The results of the simulation are presented in Figures 1, 2, and 3.

[32] The dependence of the effluent water pH on the presence of these buffering minerals in the column is clearly illustrated in Figure 1. The predicted pH is in agreement with the measured pH. However, the duration of the first pH-plateau, based on this conceptual model is too short. In addition, the modeling results suggest that an additional pH-plateau occurs at pH 4.5. This pH-plateau was not observed in the laboratory experiment. Similarly, alkalinity predicted by the reactive transport simulation occurs in two distinct steps, while laboratory measurements show a gradual decrease in alkalinity during the first 30 days (Figure 2).

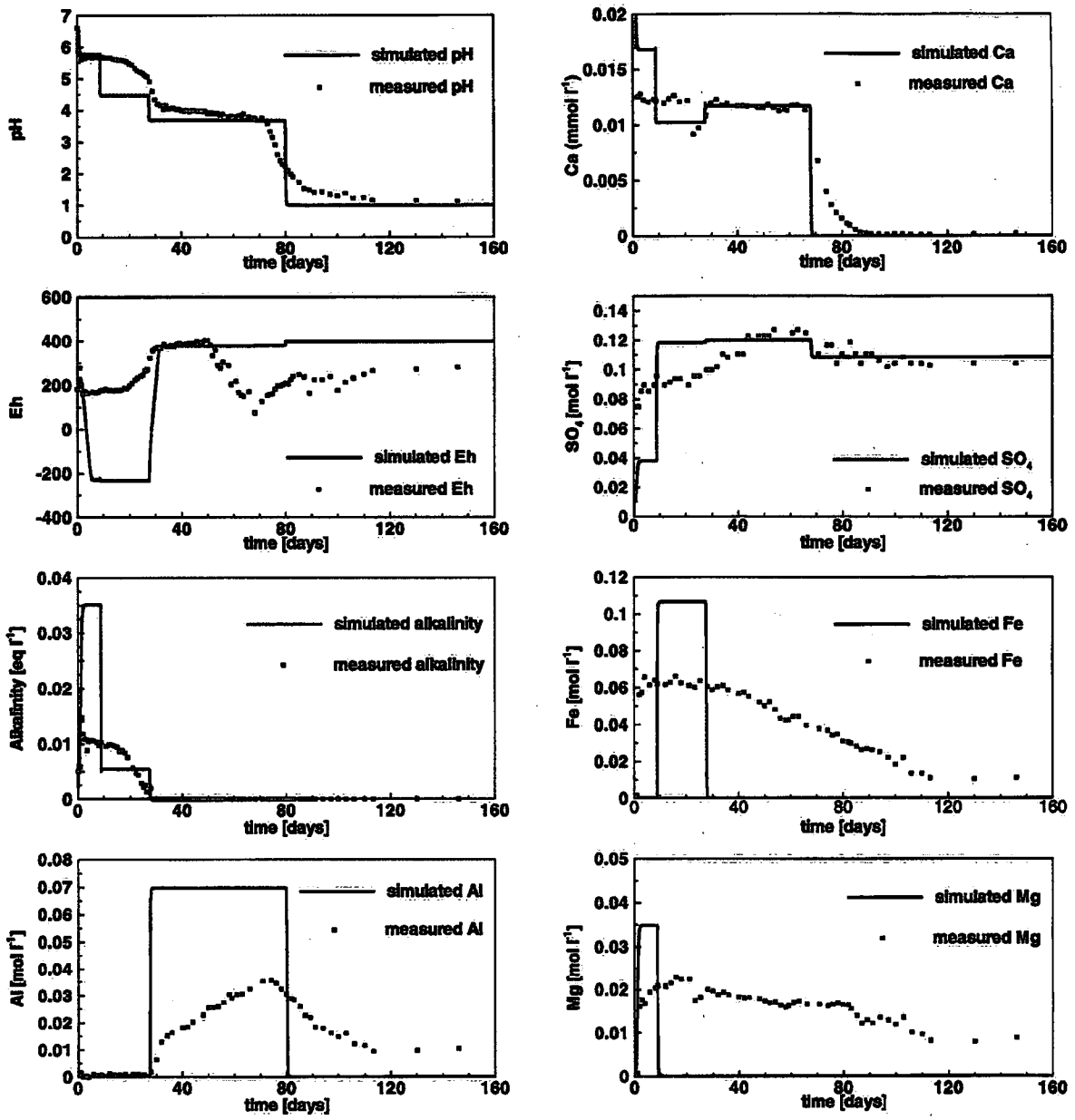

Figure 2. Step 1: Comparison of simulated and measured concentrations of major ions, pH, and Eh in the column effluent as a function of time.

Alkalinity is overpredicted during the first 10 days, while it is underpredicted between 10 and 20 days. The results of the reactive transport modeling suggest that as long as ankerite-dolomite is present in the column, the pH will remain at 5.7 (Figure 1). Upon the depletion of ankerite-dolomite from the column, the pH of the effluent water is controlled by dissolution of siderite, followed by dissolution of gibbsite at the next pH-plateau. The sequential depletion of minerals from the column is documented by plots of spatial distribution of mineral abundance at different snapshots in time (Figure 3). Modeling results suggest that 5 days after the initiation of the experiment, ankerite-dolomite has been depleted from the column at the inflow boundary side (Figure 3), while siderite has been precipitating in this area (Figure 3). During the first 5 days, a very small amount of gibbsite has dissolved at the inflow boundary side of the column. At 30 days, both carbonates have been depleted from the column. With time, the gibbsite dissolution front moves from the inflow boundary to the outflow boundary of the column, maintaining the pH at 4.0. By 80 days all the minerals contained in the conceptual model have dissolved, which is inconsistent with laboratory observations. That is, the measured effluent water pH shows that a buffering phase is still present in the column (Figure 1).

[33] The most significant discrepancy between simulated and measured parameters was observed for Fe and Mg

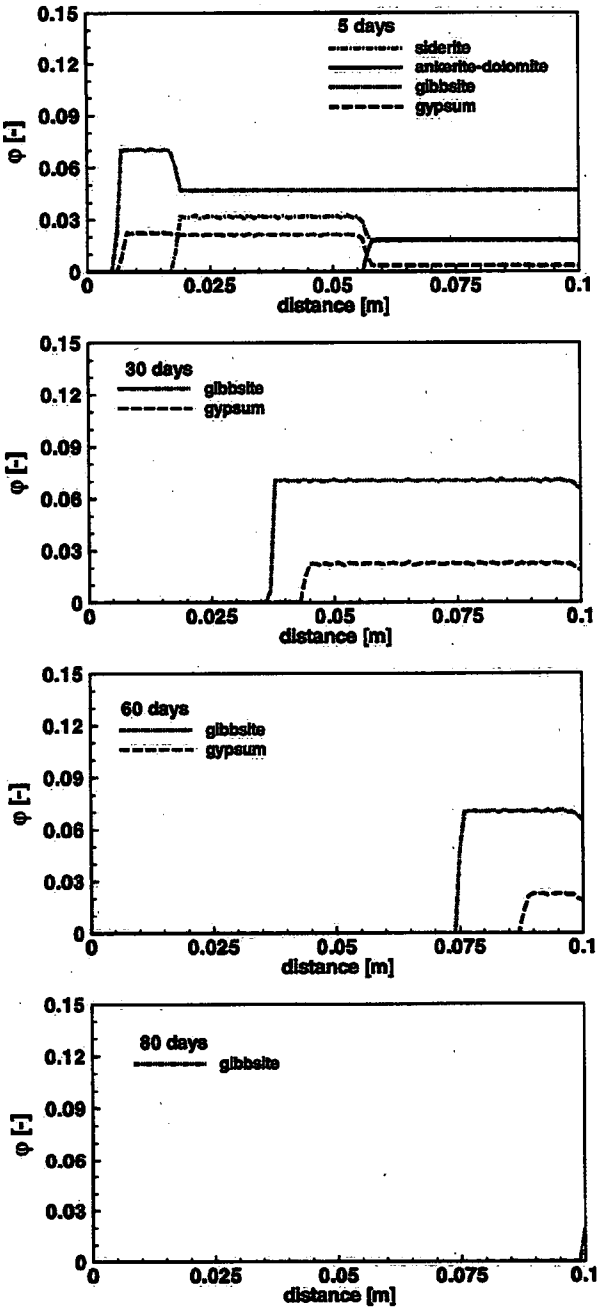

Figure 3. Step 1: Spatial distribution of mineral abundance, expressed as volume fractions, in the column at four snapshots in time: 5, 30, 60, and 80 days.

concentrations (Figure 2). The results of this simulation for Fe concentrations were inconsistent with laboratory measurements, which show very low initial concentrations in the column effluent water. The concentrations of Mg increased upon the initiation of the experiment, as observed in the effluent water of the column experiment. The discrepancies between cumulative amounts of simulated and measured Fe and Mg concentrations clearly showed that there must be an additional important source for these two elements in the tailings in addition to ankerite-dolomite and siderite. The simulated Eh values are 400 mV too low during the first 30 days, suggesting some ferric iron may have been present in the column effluent water. After 60 days, the predicted Eh is too high, which is not surprising due to the large amount of Fe not accounted for in the predicted effluent water composition (Figure 2).

[34] The simulation based on this conceptual model overpredicts the magnitude of Al concentrations in the effluent water between 30 and 75 days. In addition, observed changes in Al concentrations are not as abrupt as predicted by reactive transport modeling. The simulated Al concentrations are derived from dissolution of gibbsite. The discrepancy between the sharp increase in simulated concentrations, and the gradual increase in modeled concentrations suggests Al concentrations may not be controlled by gibbsite dissolution alone. Furthermore, a source of Al must have been present upon termination of the experiment, as Al concentrations in the column effluent water were measurable until the very end of the column experiment.

[35] The magnitude and changes in SO_4 and Ca concentrations were predicted well by the model (Figure 4). The changes in Ca and SO_4 concentrations at 75 days correspond to depletion of gypsum at the outflow boundary of the column, thereby suggesting that Ca and SO_4 concentrations were controlled by equilibrium with respect to gypsum. This observation is consistent with the results of the aqueous geochemical modeling using MINTEQA2.

4.2. Second Conceptual Model

[36] In the previous step, examination of plots generated using the equilibrium approach shows that the changes in measured parameters were more gradual than predicted by the simulation. This observation suggests that reactions controlling the major ion chemistry and pH in the effluent water were kinetically limited. Therefore the dissolution of ankerite-dolomite and siderite were considered kinetically controlled processes in the second step.

[37] An additional objective of the second step was to determine the missing source of Fe and Mg concentrations in the column effluent water. The examination of fresh Kidd Creek tailings mineralogy shows that the only substantial source of Mg and Fe besides the carbonates is chlorite (Table 3). Chlorite is also among the most rapidly dissolving of the aluminosilicates minerals present in the Kidd Creek tailings. To determine if chlorite was substantially depleted during the experiment, samples of fresh tailings, and samples of leached solids, collected at the end of the experiment, were examined to determine the changes in mineralogy. The column solids were divided in three sections from bottom to top. The comparison of peak heights of the unadjusted X-ray diffraction patterns indicates that the amount of chlorite in the tailings during the course of the experiment decreased by 60 wt.% in comparison to the amount of chlorite in fresh Kidd Creek tailings, used in the experiment (Jambor, personal communication, 2000). Therefore kinetically limited chlorite dissolution was included in the conceptual model at the second step. Gibbsite was removed from the conceptual model, as it has not been observed during the mineralogical study of the Kidd Creek tailings. Although the dissolution of gibbsite has been inferred on the basis of geochemical modeling

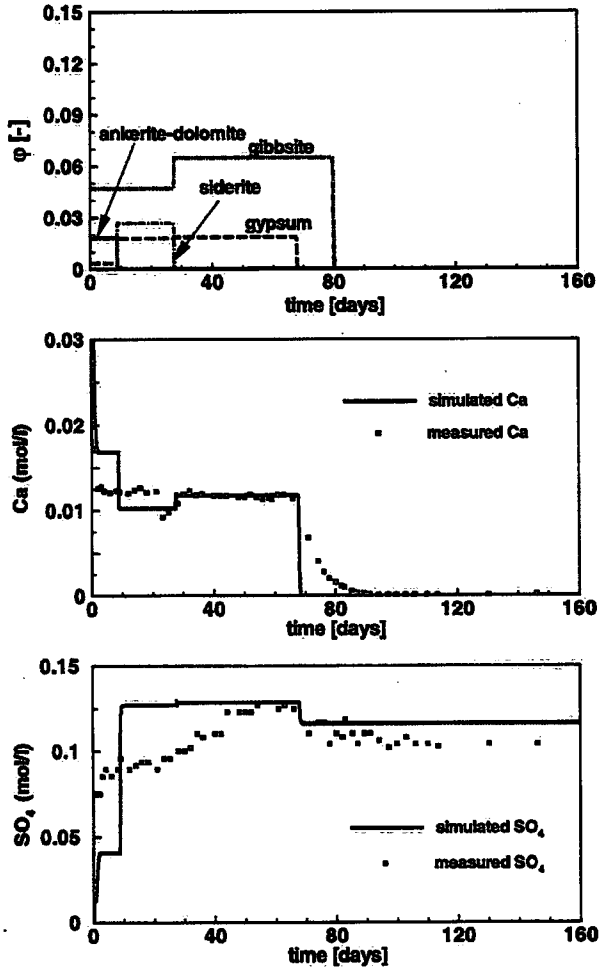

Figure 4. Step 1: Comparison of gypsum abundance at the exit boundary of the column as a function of time with Ca and SO_4 concentrations in the effluent water.

studies, its presence has not been confirmed at other tailings impoundments. Furthermore, the results of the reactive transport modeling, using the first conceptual model, suggest that 6 wt.% of gibbsite would be required to adequately explain the second pH plateau. It is likely that such an amount of the mineral would have been detected during the mineralogical study.

[38] In addition, a very small amount of ferrihydrite was included in the conceptual model to determine if dissolution of ferrihydrite would better explain the redox potential in the effluent water. Ferrihydrite was not observed in fresh Kidd Creek tailings (Table 3). However, ferrihydrite commonly occurs in tailings impoundments, and has been detected in samples of weathered tailings from the Kidd Creek site [*Al*, 1996]. Because ferrihydrite was not reported for the Kidd Creek tailings, the amount was estimated. The revised conceptual model is summarized in Table 4. The number of pH-plateaus predicted by the model is consistent with observations during the experiment (Figure 5). However, the magnitude of the second plateau in the predicted pH is higher than observed in the experiment. This discrepancy suggests that siderite does not control the pH at the second plateau.

[39] The inclusion of chlorite into the conceptual model was able to provide Fe, Mg, and Al in the later stages of the experiment (Figure 6). However, there is a much larger discrepancy in predicted and measured pH on the basis of this conceptual model than in step one (Figure 1). The results of the modeling show that the larger amount of Fe, present in the conceptual model at the second step derived from chlorite dissolution, resulted in precipitation of a large mass of siderite. Therefore the predicted pH of the effluent water remains at 4.5 until 80 days. It is unlikely that the pH of the effluent water would have been controlled by siderite during the first 80 days of the experiment due to discrepancies in the shapes of the simulated alkalinity curve, and measured alkalinity. The depletion of siderite from the column corresponds to the beginning of the decrease in the chlorite content at the outflow boundary of the column. The simulation predicts that, during the first 80 days of the experiment, roughly 60 wt% of chlorite has been removed from the column; while at the end of the experiment at 150 days roughly 50 wt% of chlorite remains in the column (Figure 7). This prediction is in reasonable agreement with the observations reported by Jambor (personal communication, 2000). On the basis of unadjusted XRD patterns for the leached tailings, collected after the experiment, Jambor concluded that 40% chlorite remained in the leached tailings.

[40] Kinetically limited dissolution of chlorite also provides a better prediction of Al concentrations in the effluent water (Figure 6). Changes in predicted Al concentrations are more gradual in comparison to step 1, which is more consistent with Al concentrations measured experimentally. In addition, the magnitude of predicted Al concentrations is

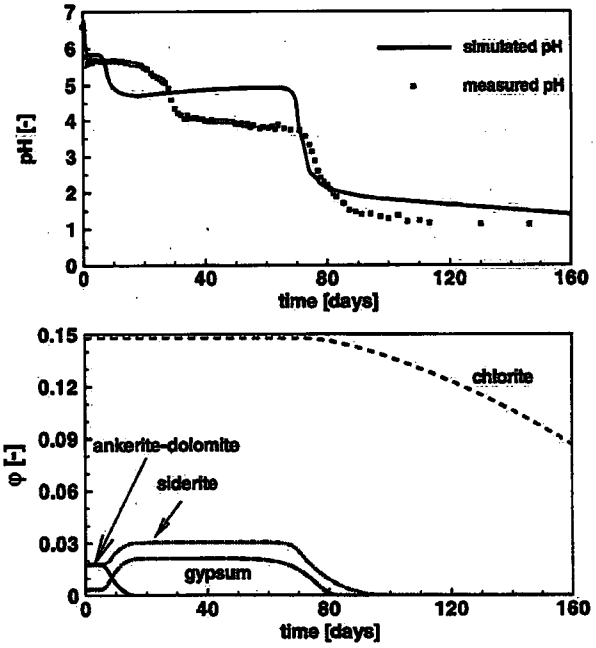

Figure 5. Step 2: Comparison of pH and abundance of minerals, expressed as volume fractions, at the outflow boundary of the column as a function of time.

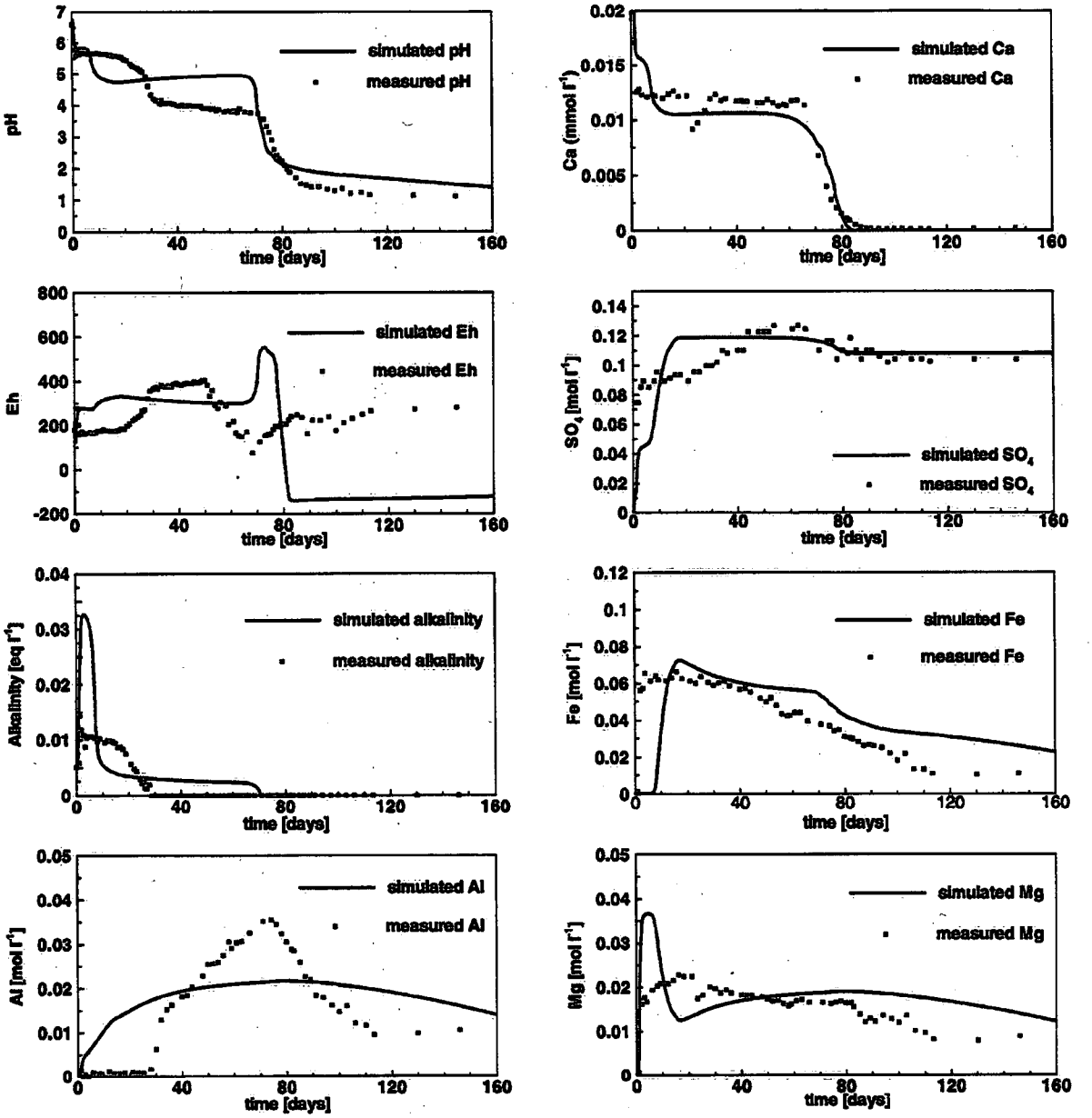

Figure 6. Step 2: Comparison of simulated and measured concentrations of major ions, pH, and Eh in the column effluent as a function of time.

in better agreement with those observed in the laboratory. The largest discrepancy between measured and predicted Al concentrations occurs during the first 30 days of the experiment.

[41] The first change in Eh corresponds to the first change in pH where the concentration of Fe(III) increases substantially due to the dissolution of ferrihydrite (Figure 8). In comparison to step 1, the simulation results for Ca and SO_4 fit the data equally well.

4.3. Third Conceptual Model

[42] In the second step, gibbsite was removed from the conceptual model because it was not reported in mineralogical analyses of fresh Kidd Creek tailings sample (Table 3). However, the simulated pH curve in the second step deviates more from the measured pH curve than in the first step. That is, the simulation does not predict a pH plateau at a value of 4.0, which was very long and distinct in the laboratory measurements. Furthermore, a plateau of pH at a value of 4.0 has been observed at a number of field sites, for example, at Heath Steele, New Brunswick [*Blowes et al.*, 1991], and at the Nickel Rim tailings impoundment [*Johnson et al.*, 2000]. Aqueous geochemical modeling of water effluent samples using MINTEQA2 suggests equilibrium with respect to gibbsite at the second pH plateau. This observation is consistent with the conceptual acid neutral-

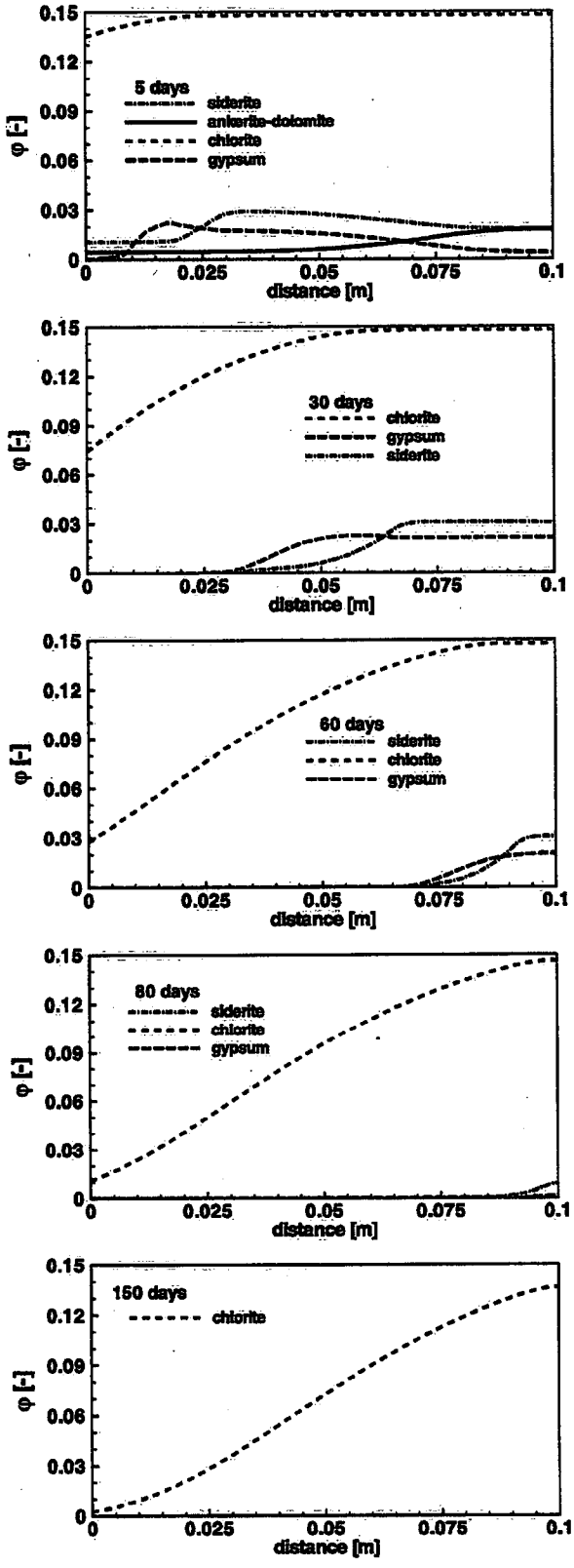

Figure 7. Step 2: Spatial distribution of mineral abundance, expressed as volume fractions, in the column at five snapshots in time: 5, 30, 60, 80, and 150 days.

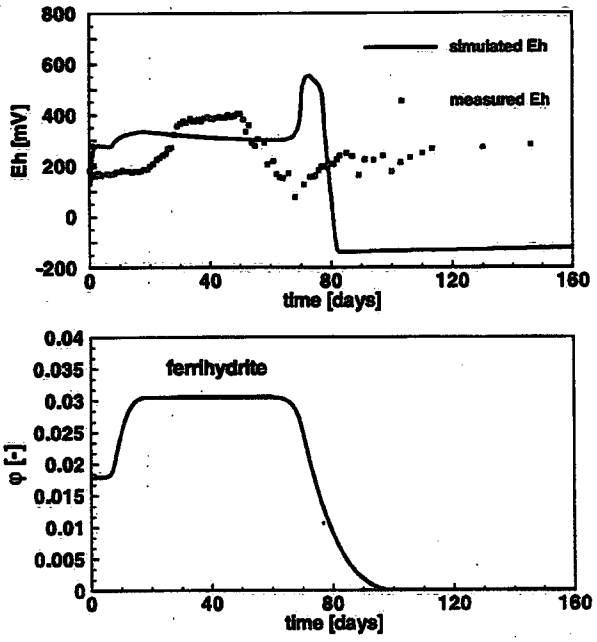

Figure 8. Step 2: Comparison of Eh and abundance of ferrihydrite at the outflow boundary of the column.

ization model [*Blowes and Ptacek*, 1994; *Morin et al.*, 1988]. According to the conceptual model, gibbsite precipitates from the tailings pore water due to high Al concentrations, which are derived from aluminosilicate dissolution. In the case of Kidd Creek tailings, most Al is derived from chlorite due to its abundance and rapid rate of dissolution.

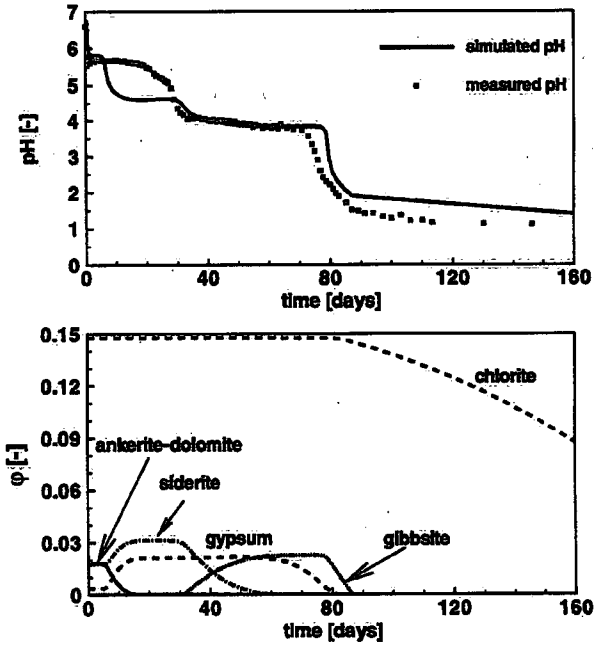

Figure 9. Step 3: Comparison of pH and abundance of minerals, expressed as volume fractions, at the outflow boundary of the column as a function of time.

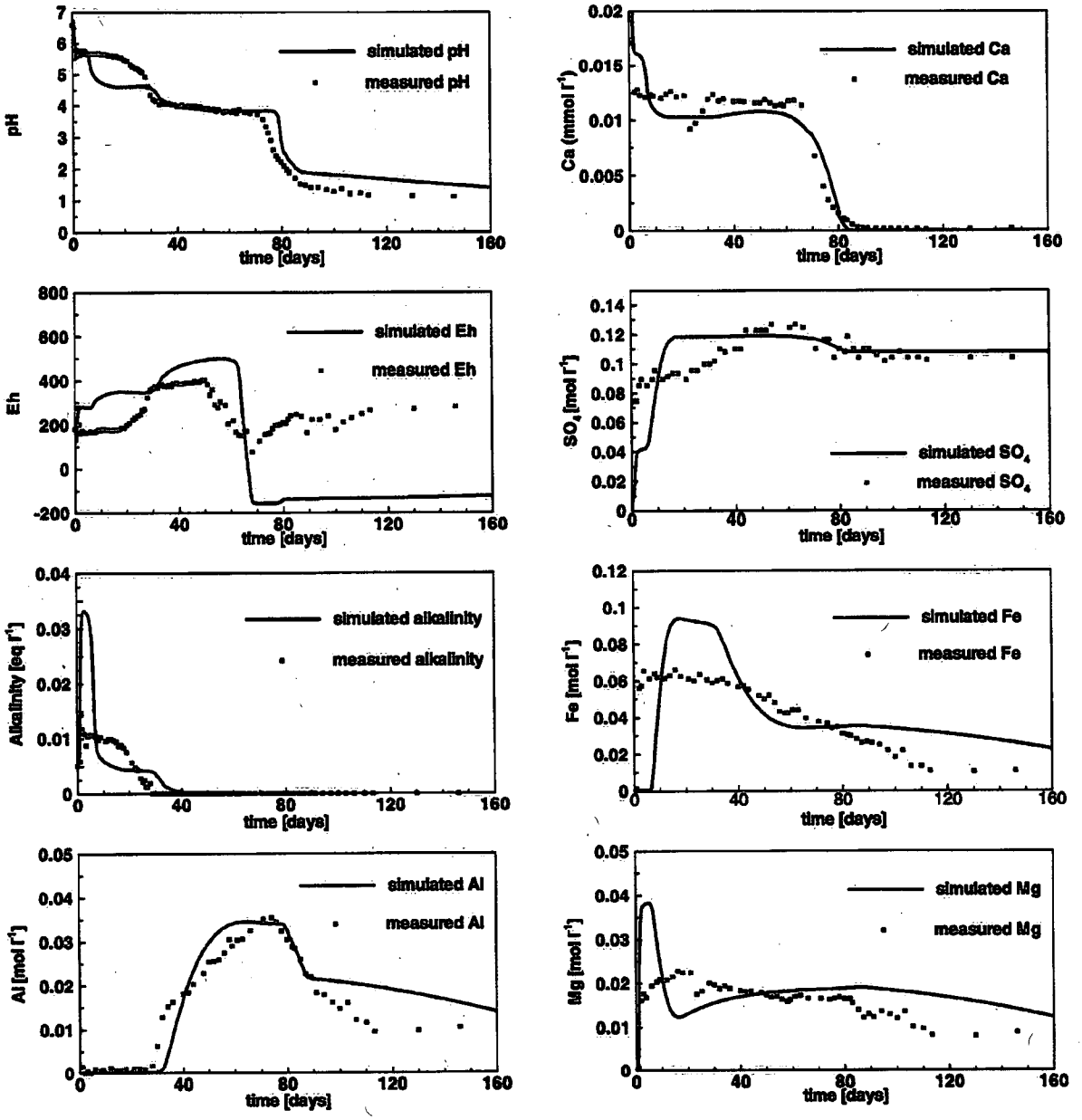

Figure 10. Step 3: Comparison of simulated and measured concentrations of major ions, pH, and Eh in the column effluent as a function of time.

Therefore gibbsite was reintroduced to the conceptual model used in the third step (Table 4). The results of the simulation are presented in Figures 9, 10, 11, and 12.

[43] The predicted pH curve, on the basis of the third conceptual model, is in better agreement with the measured pH curve than in steps one and two (Figure 9). The magnitude of the first and third predicted pH plateaus correspond well to observed data, and the changes in pH are more gradual than in step 1, as observed in the laboratory experiment. However, a pH plateau at 4.5 is still present, which was not observed in the laboratory column experiment. The examination of Figure 9 reveals that the pH at the plateau of 4.5 is controlled by siderite dissolution. This observation suggests that siderite precipitation and dissolution may not have been a major control on pore water pH in the laboratory experiment. This observation is supported by the discrepancy in predicted and measured Fe concentrations at the beginning of the experiment (Figure 10), where the predicted concentrations of Fe are very low due to siderite precipitation in the column.

[44] The gradual changes in pH are accompanied by a gradual depletion of buffering minerals in the column (Figure 9). The simulation results suggest that a minor amount of ankerite-dolomite is still present at the outflow boundary of the column when pH decreases from 5.7 to 4.5. Similarly, a small amount of siderite is present at the end of

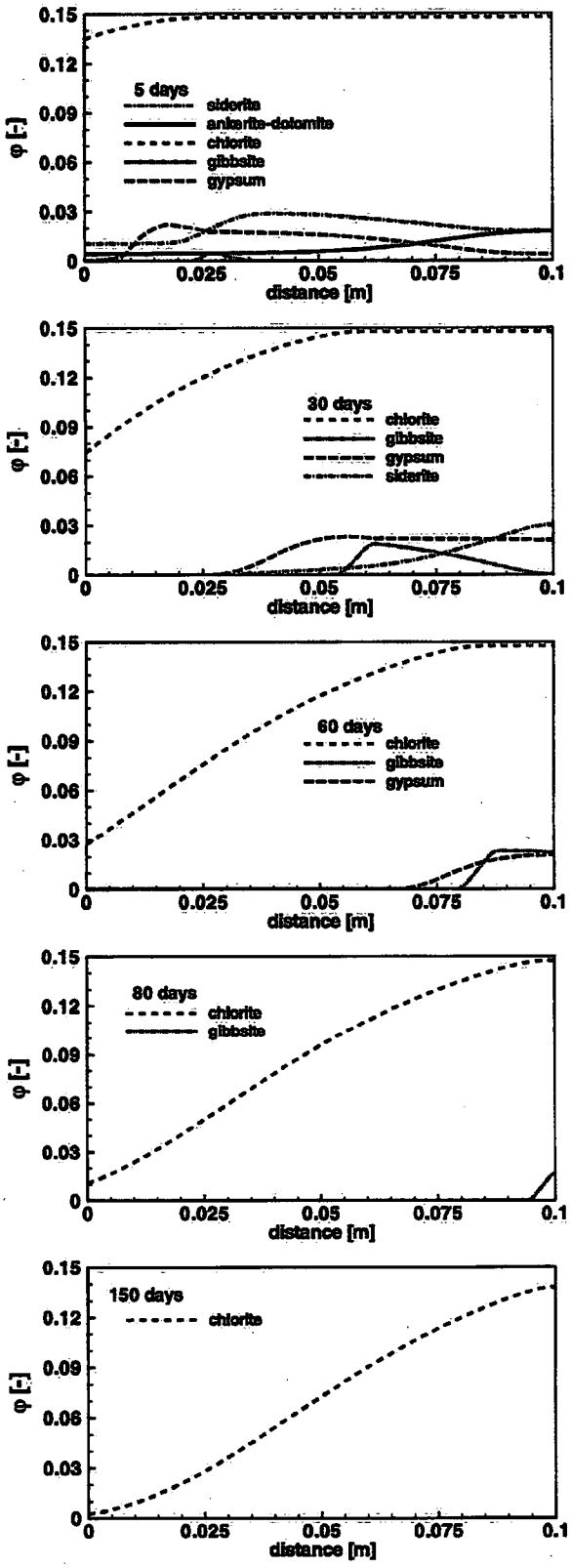

Figure 11. Step 3: Spatial distribution of mineral abundance, expressed as volume fractions, in the column at five snapshots in time: 5, 30, 60, 80, and 150 days.

the column when pH changes from 4.5 to 4.0. This prediction is consistent with field observations of *Johnson et al.* [2000] at the Nickel Rim mine tailings impoundment, who found that the carbonate content in the tailings decreased in solid samples by an order of magnitude where the pore water pH decreased below 4.5. The predicted change in carbonate content (Figure 9) using MIN3P is not as abrupt as the observation of *Johnson et al.* [2000] in the field. The discrepancy can be attributed to the differences in the flow rate in the laboratory column experiment and flow rates observed in the field. The flow rate in the laboratory experiment was one order of magnitude faster than the average flow rate observed in the field settings.

[45] Addition of gibbsite to the conceptual model as a secondary mineral, which can precipitate during the experiment, significantly improved the prediction of Al concentrations in the effluent water (Figure 10). The shape of the predicted alkalinity curve is similar to the shape of alkalinity based on the first conceptual model. That is, the shape of the alkalinity curve is still inconsistent with laboratory measurements. Furthermore, the shapes of predicted Fe and Mg concentrations at the beginning of the experiment are still inconsistent with those observed in the laboratory. The initial predicted Fe concentrations are 0.6 mol/l too low, and are followed by over predicted Fe concentrations. On the contrary, predicted Mg concentrations at the beginning of the experiment are too high. Predicted Eh, on the basis of the third conceptual model, is in much better agreement with the laboratory measurements of Eh than in step one and two (Figure 12). Ca and SO_4 again remain unaffected by the revised conceptual model and correspond relatively well to the observed data.

[46] The examination of Figure 11 shows that the amount of precipitated gibbsite is very small. In addition, the

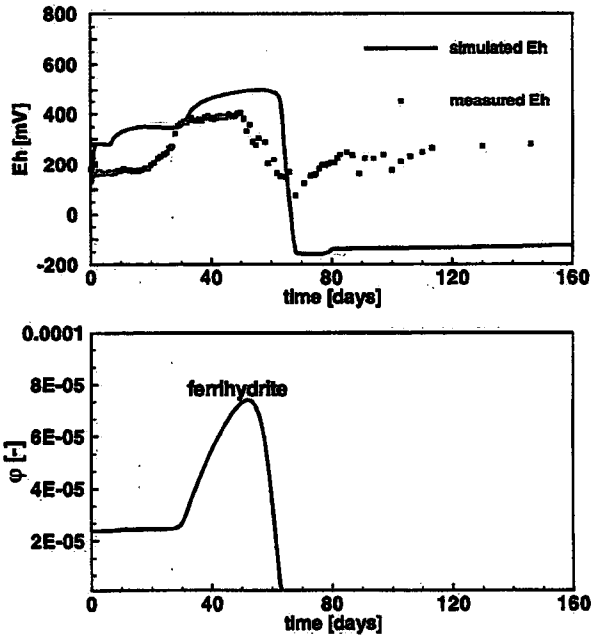

Figure 12. Step 3: Comparison of Eh and abundance of ferrihydrite, expressed as volume fractions, at the outflow boundary of the column.

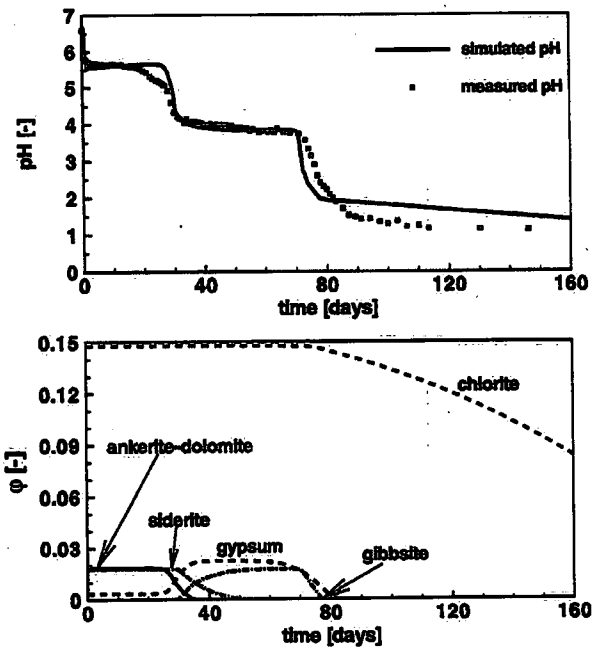

Figure 13. Step 4: Comparison of pH and abundance of minerals, expressed as volume fractions, at the outflow boundary of the column as a function of time.

location of precipitated gibbsite moves quickly through the column. This result suggests that the identification of an Al secondary phase would be difficult.

4.4. Fourth Conceptual Model

[47] The focus of the fourth step was to construct a model, which would correctly predict the observed pH. In step three, it was shown that the pH of the plateau at 4.5 is controlled by siderite. Therefore no siderite was allowed to precipitate in the fourth step. This assumption is reasonable considering the relatively fast flow rate in the column in comparison to field situations. The assumption of inhibited siderite precipitation is in agreement with observations of *Greenberg and Thomson* [1992], who determined in their experiments that the rate of siderite precipitation is 100 times slower than for any other 2:2 sparingly soluble salt. The conceptual model, used in the fourth step, is summarized in Table 4.

[48] Kinetically limited dissolution of primary ankerite-dolomite, siderite, chlorite and secondary gibbsite precipitation and redissolution provides favorable agreement with measured pH (Figure 13). The results of the reactive transport modeling indicate that ankerite-dolomite is depleted roughly ten days earlier than siderite, which is consistent with the gradual decrease in measured and predicted pH (Figure 13). Modeling results suggest that the presence of minor amounts of siderite at the end of the column after 40 days of the experiment may be the reason for the

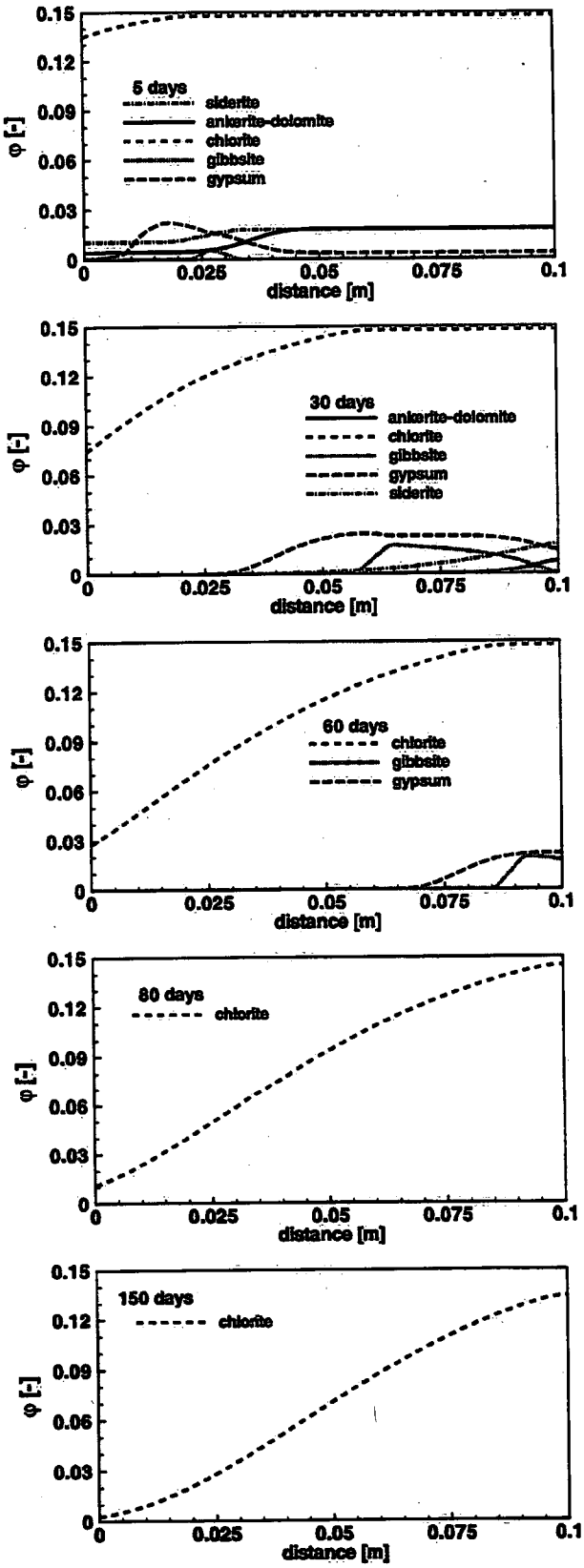

Figure 14. Step 4: Spatial distribution of mineral abundance in the column at five snapshots in time: 5, 30, 60, 80, and 150 days. The abundance of minerals is expressed in volume fraction.

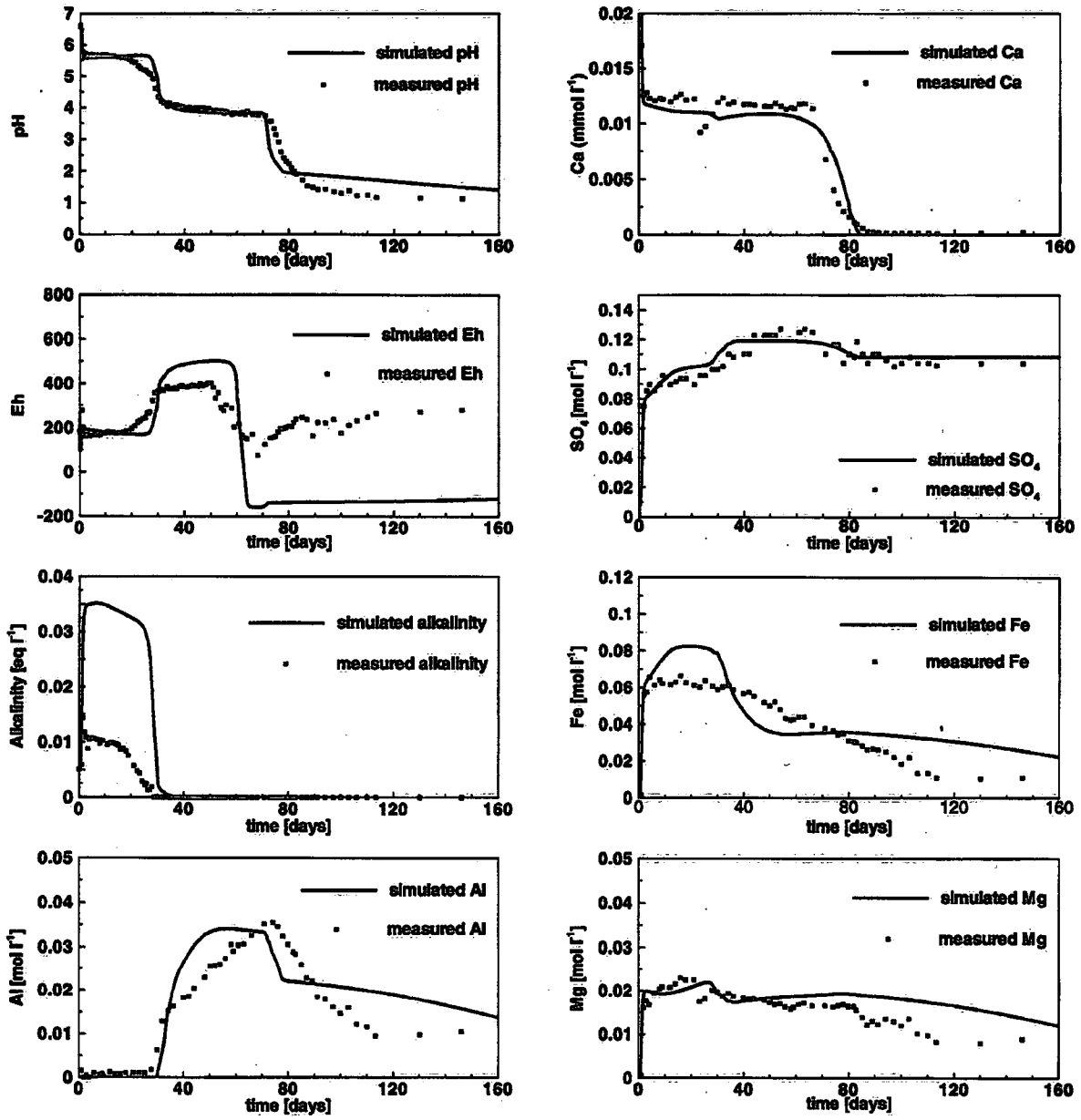

Figure 15. Step 4: Comparison of simulated and measured concentrations of major ions, pH, and Eh in the column effluent as a function of time.

slight inclination of the second pH plateau (Figure 13). Because siderite was not allowed to precipitate in this step, the depletion of ankerite-dolomite was slower than in the third step (Figures 14 and 11), which maintains the pH at 5.7 for a longer time. The depletion of gibbsite from the column after 80 days corresponds to the second decrease in pH and roughly 60% depletion of chlorite from the column (Figure 13).

[49] The predicted shape of the alkalinity curve is very similar to the laboratory measurements (Figure 15). However, the magnitude of predicted alkalinity is three times higher than the measured alkalinity in the effluent water. This prediction could potentially be explained by laboratory observations, where a substantial amount of gas was observed to pass through the sampling cell as long as pH remained 5.7. No gas formed at later stages of the experiment. The CO_2 degassing was not modeled, as there are no laboratory data of the pressure distribution in the column or the hydraulic conductivity.

[50] The simulated Mg and Fe concentrations are in better agreement with those measured in the laboratory than in the third step in which siderite was allowed to precipitate. In addition, the magnitude of the abrupt increase in SO_4 concentrations at the beginning of the experiment is in better agreement with the laboratory observations as well as the match for Ca (Figures 10 and 15). Better agreement

of predicted and measured pH, also enabled better prediction of Eh values in the effluent water (Figure 16). After 80 pore volumes the simulated Eh does not match the laboratory data as well in the first part of the experiment. The discrepancy is likely due to an unrepresented source of ferric iron in the simulations. Minor amounts of ferric iron could be coming from chlorite, or from the dissolution of pyrrhotite.

[51] The predicted Al concentrations are unchanged from the third step. The predicted concentrations of Al start to deviate from those measured in the effluent water at about 80 days (Figure 15). At the same time, pH predicted by MIN3P is slightly too high. At this time, the most rapidly dissolving mineral in the column is chlorite, which controls the pH of the effluent water (Figure 13). The deviation of simulated from measured Al concentrations is consistent with slightly higher predicted concentrations of Fe and Mg than observed in the laboratory. The results indicate, that the simulation predicts dissolution of chlorite at low pH earlier than observed in the laboratory.

[52] The concentrations of Al, Fe and Mg, as well as pH start to deviate at 80 days, when predicted pH is 2. The rate expression for chlorite was only tested for pH values above 3. Therefore the discrepancies in concentrations of components derived from chlorite may be due to an incorrect rate expression for pH values less than 2.

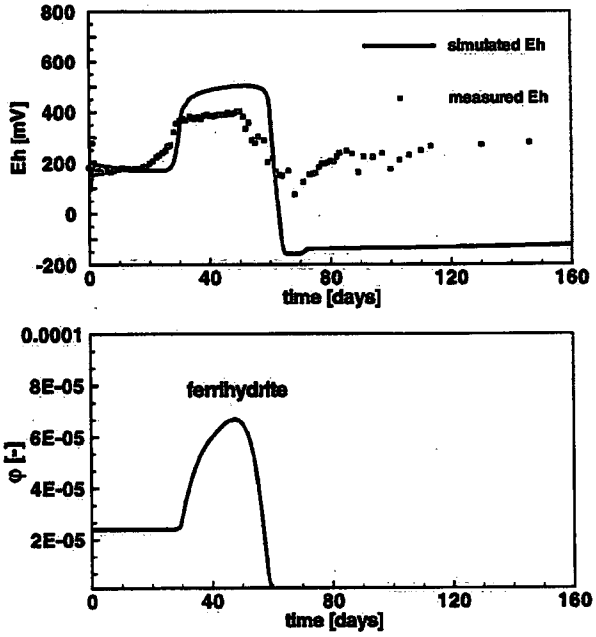

Figure 16. Step 4: Comparison of Eh and abundance of ferrihydrite, expressed as volume fractions, at the outflow boundary of the column.

5. Summary and Conclusions

[53] This study presents an attempt in modeling pH changes due to acid neutralization reactions in a mine tailings environment for which a large database exists. The simulations were constrained by the amounts of minerals that were determined by an independent mineralogical study. A conceptual model that adequately predicts the measured pH in the column effluent water consisted of dissolution reactions including ankerite-dolomite, siderite and chlorite in conjunction with the precipitation and redissolution of secondary gibbsite. The results of the reactive transport modeling reproduce the dissolution of the carbonates during the first 30 pore volumes of the experiment. The observed amount of chlorite dissolved during the experiment is in reasonable agreement with the modeling results. The simulated concentrations of Ca, SO_4, Fe, Mg and Al are also in good agreement with the measured concentrations. Modeling results suggest that dissolution and precipitation of gypsum control the concentrations of Ca and SO_4 in the column effluent water, while the inferred dissolution of a small amount of ferrihydrite in addition to other Fe-bearing phases, namely ankerite-dolomite, siderite and chlorite, can explain the redox potential of the effluent water. The final simulation based on the fourth conceptual model suggests that substantial amounts of siderite did not precipitate in the column experiment. This modeling result suggests that the siderite solubility product limited Fe concentrations through dissolution only. The kinetically limited dissolution of chlorite appears to contribute the largest mass of Mg and Fe (II) to the effluent water, followed by ankerite-dolomite, which contributes substantially less.

[54] The modeling results suggest that numerical simulations can be in good agreement with observations from the laboratory, when parameters and sufficient information about the system are available. The agreement between simulated and measured concentrations, in addition to the consistency of the amounts of minerals used in the simulations with those observed in mineralogical analyses, is encouraging; especially considering that the model does not support incongruent dissolution nor has the chlorite rate expression been tested for solutions with pH below 3.0. Therefore the simulated reaction rates occurring at pH less than 3.0 may not reflect the reaction rates occurring in the laboratory column experiment. In addition, the chlorite rate expression was not tested for high SO_4 content, which might affect the rate of release of Al. On the basis of observations of enhanced release of Al from gibbsite, it has been speculated that precipitation-dissolution reaction rates of minerals containing Al may be more rapid in solutions containing SO_4 [*Ridley et al.*, 1997].

[55] The differences between the simulation results based on the second and third conceptual model illustrate that it is likely that pH at the second pH plateau and Al concentrations in the effluent water are controlled by a secondary Al phase, possibly gibbsite or another Al phase with a solubility similar to gibbsite. Our results are consistent with observations at many tailings impoundments [*Blowes*, 1990; *Dubrovsky et al.*, 1985; *Johnson et al.*, 2000; *Morin et al.*, 1988] where equilibrium with respect to gibbsite has been suggested based on geochemical equilibrium calculations. Furthermore, chemical analyses of weathered tailings from the oxidized zone of tailings impoundments show accumulation of Al [*Blowes*, 1990; *Johnson*, 1993], although the secondary aluminum phase has not yet been identified by mineralogical analyses. The results of these simulations suggest that a secondary Al phase occurs in very small quantities over

a narrow time interval, which makes the search for the phase even more difficult. The search for the secondary Al phase, controlling Al concentrations in weathering environments is not restricted to mine tailings. In soil science, the present-day view on the predominant secondary mineral phase acting as Al solubility control has been divided between proponents of Al in equilibrium with (1) gibbsite, (2) a metastable aluminum phase and (3) a mixed phase of fast-reacting aluminum hydroxide and aluminosilicate [*Ducet et al.*, 2001]. Possible dissolution/precipitation reactions of the metastable aluminum phase and the mixed phase of fast-reacting aluminum hydroxide and aluminosilicate have not been simulated in this study due to lack of thermodynamic data and because there is no evidence of the formation of these phases in mine tailings environment. More research is needed to resolve the question of Al control in tailings pore water and buffering of tailings pore water pH to 4.0.

References

Al, T. A. (1996), The hydrology and geochemistry of thickened, sulfide-rich tailings, Kidd Creek Mine, Timmins, Ontario, Ph.D. Univ. of Waterloo, Dep. of Earth Sci., Waterloo, Ontario, Canada.

Allison, J. D., D. S. Brown, and K. J. Novo-Gradac (1990), MINTEQA2/PRODEFA2, a geochemical assessment model for environmental systems, version 3.0 user's manual, 106 pp., Environ. Res. Lab., U.S. Environ. Prot. Agency, Athens, Ga.

Appelo, C. A. J., and D. Postma (1999a), A consistent model for surface complexation on birnessite (δ-MnO_2) and its application to a column experiment, *Geochim. Cosmochim. Acta*, *63*(19/20), 3039–3048.

Appelo, C. A. J., and D. Postma (1999b), Variable dispersivity in a column experiment containing MnO_2 and FeOOH coated sand, *J. Contam. Hydrol.*, *40*, 95–106.

Ball, J. W., and D. K. Nordstrom (1991), Users manual for WATEQ4F, with revised thermodynamic data base and test cases for calculating speciation of major trace, and redox elements in natural water, *U.S. Geol. Surv. Open File Rep.*, *91-183*.

Blowes, D. W. (1990), The geochemistry, hydrogeology and mineralogy of decommissioned sulfide tailings: A comparative study, Ph.D., Univ. of Waterloo, Waterloo, Ontario, Can.

Blowes, D. W., and C. J. Ptacek (1994), Acid-neutralization mechanisms in inactive mine tailings, in *The Environmental Geochemistry of Sulfide Mine-Wastes*, edited by D. W. Blowes and J. L. Jambor, *Short Course Handb. Mineral. Assoc. Can.*, *22*, 271–292.

Blowes, D. W., E. J. Reardon, J. L. Jambor, and J. A. Cherry (1991), The formation and potential importance of cemented layers in inactive sulfide mine tailings, *Geochim. Cosmochim. Acta*, *55*, 965–978.

Blum, A. E., and L. L. Stillings (1995), *Feldspar Dissolution Kinetics*, edited by A. F. White and S. L. Brantley, *Rev. Mineral.*, *31*, 291–352.

Bredehoeft, J. D., and P. Hall (1995), Ground-water models, *Ground Water*, *33*(4), 530–531.

Bredehoeft, J. D., and L. F. Konikow (1993), Ground-water models: Validate or invalidate, *Ground Water*, *31*(2), 178–179.

Chilakapati, A., T. Ginn, and J. Szecsody (1998), An analysis of complex reaction networks in groundwater modeling, *Water Resour. Res.*, *34*(7), 1767–1780.

Dubrovsky, N. M., J. A. Cherry, and E. J. Reardon (1985), Geochemical evolution of inactive pyritic tailings in the Elliot Lake uranium district, *Can. Geotech. J.*, *22*, 110–128.

Ducet, F. J., C. Schneider, S. J. Bones, A. Kretchmer, I. Moss, P. Tekely, and C. Exley (2001), The formation of hydroxyaluminosilicates of geochemical and biogeochemical significance, *Geochim. Cosmochim. Acta*, *65*(15), 2461–2467.

Glynn, P. D., and J. Brown (1996), Reactive transport modeling of acid metal-contaminated groundwater at a site with sparse spatial information, edited by P. C. Lichtner, C. I. Steefel, and E. H. Oelkers, *Rev. Mineral.*, *34*, 377–436.

Greenberg, J., and M. Thomson (1992), Precipitation and dissolution kinetics and equillibria of aqueous ferrous carbonate vs. temperature, *Appl. Geochem.*, *7*, 185–190.

Guha, H., J. E. Saiers, S. Brooks, P. Jardine, and K. Jayachandran (2001), Chromium transport, oxidation, and adsorption on manganese-coated sand, *J. Contam. Hydrol.*, *49*, 311–334.

Jambor, J. L. (1994), Mineralogy of sulfide-rich tailings and their oxidation products, in *Environmental Geochemistry of Sulfide Mine-Wastes*, edited by J. L. Jambor and D. W. Blowes, *Short Course Handb. Mineral. Assoc. Can.*, *22*, 59–102.

Jambor, J. L., and D. W. Blowes (1998), Theory and applications of mineralogy in environmental studies of sulfide-bearing mine tailings, in *Modern Approaches to Ore and Environmental Mineralogy*, *Short Course Ser.*, vol. 12, edited by L. J. Cabri and D. J. Vaughan, pp. 376–401, Mineral. Assoc. of Can., Ottawa, Ontario.

Jambor, J. L., D. R. Owens, P. Carriere, and R. Lastra (1993), Mineralogical investigation of tailings and associated waste products, and the distribution of natrojarosite in the Kidd Creek Main Tailings Cone, Timmins, Ontario, *Miner. Sci. Lab. Div. Rep. MSL 93-20 (CR)*, 198 pp., Can. Cent. for Miner. and Energy Technol., Ottawa, Ontario.

Jaynes, D. B., H. B. Pionke, and A. S. S. Rogowski (1984), Acid mine drainage from reclaimed coal strip mines: 2. Simulation reults of the model, *Water Resour. Res.*, *20*(2), 243–250.

Johnson, R. H. (1993), The physical and chemical hydrogeology of the Nickel Rim mine tailings, Sudbury, Ontario, M.Sc., 108 pp., Univ. of Waterloo, Waterloo, Ontario.

Johnson, R. H., D. W. Blowes, W. D. Robertson, and J. L. Jambor (2000), The hydrogeochemistry of the Nickel Rim mine tailings impoundment, Sudbury, Ontario, *J. Contam. Hydrol.*, *41*, 49–80.

Jurjovec, J., C. J. Ptacek, and D. W. Blowes (2002), Acid neutralization mechanisms and metal release in mine tailings: A laboratory column experiment, *Geochim. Cosmochim. Acta*, *66*(9), 1511–1523.

Klein, C., and C. Hurlbut (1993), *Manual of Mineralogy*, 21st ed., 640 pp., John Wiley, Hoboken, N. J.

Konikow, L. F., and J. D. Bredehoeft (1992), Ground-water models cannot be validated, *Adv. Water Resour.*, *15*, 75–83.

Liu, C. W., and T. N. Narashimhan (1989), Redox controlled multiple-species reactive chemical transport: 1. Model development, *Water Resour. Res.*, *25*(5), 868–882.

Lowson, R. T., M. C. J. Comarmond, G. Rajaratnam, and P. L. Brown (2004), The kinetics of the dissolution of chlorite as a function of pH and at 25C, *Geochim. Cosmochim. Acta*, in press.

Lüttge, A., U. Winkler, and A. C. Lasaga (2003), Interferometric study of the dolomite dissolution: A new conceptual model for mineral dissolution, *Geochim. Cosmochim. Acta*, *67*(6), 1099–1116.

Mayer, K. U., S. G. Benner, and D. W. Blowes (1999), The reactive transport model MIN3P: Application to acid mine drainage generation and treatment—Nickel Rim Mine Site, Sudbury, Ontario, paper presented at Sudbury '99, Conference on Mining and the Environment, Laurentian Univ. Sudbury, Ontario, Canada.

Mayer, K. U., E. O. Frind, and D. W. Blowes (2002), Multicomponent reactive transport modeling in variably saturated porous media using a generalized formulation for kinetically controlled reactions, *Water Resour. Res.*, *38*(9), 1174, doi:10.1029/2001WR000862.

Morin, K. A., and J. A. Cherry (1986), Trace amounts of siderite near a uranium-tailings impoundment, Elliot lake, Ontario, Canada, and its implication in controlling contaminant migration in a sand aquifer, *Chem. Geol.*, *56*, 117–134.

Morin, K. A., J. A. Cherry, N. K. Dave, T. P. Lim, and A. J. Vivyurka (1988), Migration of acidic groundwater seepage from uranium-tailings impoundments, 1. Field study and conceptual hydrogeochemical model, *J. Contam. Hydrol.*, *2*, 271–303.

Oreskes, N., and B. K. Shrader-Frechette (1994), Verification, validation and confirmation of numerical models in the Earth sciences, *Science*, *263*, 641–646.

Parker, J. C., and M. T. van Genuchten (1994), Determining transport parameters from laboratory and field tracer experiments, *Bull. Va. Agric. Exp. Stn.*, *84-3*, 97 pp.

Parkhurst, D. L., and C. A. J. Appelo (1999), User's guide to PHREEQC (version 2)—A computer program for speciation, batch-reaction, one-dimensional transport, and inverse geochemical calculations, *U.S. Geol. Surv. Water Resour. Invest. Rep.*, *99-4259*, 312 pp.

Ridley, M. K., D. J. Wesolowski, D. A. Palmer, P. Bénézeth, and R. M. Kettler (1997), Effect of sulfate on the release rate of Al^{3+} from gibbsite in low-temperature acidic waters, *Environ. Sci. Technol.*, *31*, 1925–1992.

Saiers, J. E., H. Guha, P. Jardine, and S. Brooks (2000), Development and evaluation of a mathematical model for the transport and oxidation-reduction of CoEDTA, *Water Resour. Res.*, *36*, 3151–3165.

Singer, P. C., and W. Stumm (1970), Acid mine drainage: The rate-determining step, *Science*, *167*, 1121–1123.

Slack, J. F., and P. R. Coad (1989), Multiple hydrothermal and metamorphic events in the Kidd Creek volcanogenic massive sulphide deposit, Timmins, Ontario: Evidence from tourmalines and chlorites, *Can. J. Earth Sci.*, *26*, 694–715.

Steefel, C. I., and P. Van Cappellen (1998), Reactive transport modeling of natural systems, *J. Hydrol.*, *209*, 1–7.

Walter, A. L., E. O. Frind, D. W. Blowes, C. J. Ptacek, and J. W. Molson (1994), Modeling of multicomponent reactive transport in groundwater: 2. Metal mobility in aquifers impacted by acidic mine tailings discharge, *Water Resour. Res.*, *30*(11), 3149–3158.

White, A. F., and L. N. Plummer (1990), Role of reactive-surface-area characterization in geochemical kinetic models, in *Chemical Modeling of Aqueous Systems II*, *ACS Symp. Ser.*, *35*, 460–475.

D. W. Blowes and J. Jurjovec, Department of Earth Sciences, University of Waterloo, Waterloo, Ontario, Canada N2L 3G1. (jjurjove@sympatico.ca)

K. U. Mayer, Department of Earth and Ocean Sciences, University of British Columbia, Vancouver, BC, Canada V6T 1Z4.

C. J. Ptacek, National Water Research Institute, Environment Canada, Burlington, Ontario, Canada L7R 4A6.

Environment Canada Environnement Canada

Canada

Canada Centre for Inland Waters
P.O. Box 5050
867 Lakeshore Road
Burlington, Ontario
L7R 4A6 Canada

National Hydrology Research Centre
11 Innovation Boulevard
Saskatoon, Saskatchewan
S7N 3H5 Canada

St. Lawrence Centre
105 McGill Street
Montreal, Quebec
H2Y 2E7 Canada

Place Vincent Massey
351 St. Joseph Boulevard
Gatineau, Quebec
K1A 0H3 Canada

Centre canadien des eaux intérieures
Case postale 5050
867, chemin Lakeshore
Burlington (Ontario)
L7R 4A6 Canada

Centre national de recherche en hydrologie
11, boul. Innovation
Saskatoon (Saskatchewan)
S7N 3H5 Canada

Centre Saint-Laurent
105, rue McGill
Montréal (Québec)
H2Y 2E7 Canada

Place Vincent-Massey
351 boul. St-Joseph
Gatineau (Québec)
K1A 0H3 Canada